



RESEARCH LETTER

10.1029/2021GL094074

Joint Dependence of Longwave Feedback on Surface Temperature and Relative Humidity

Brett A. McKim¹ , Nadir Jeevanjee² , and Geoffrey K. Vallis¹

¹University of Exeter, Exeter, UK, ²Geophysical Fluid Dynamics Laboratory, Princeton, NJ, USA

Key Points:

- The longwave clear-sky feedback exhibits a significant relative humidity dependence at high temperatures
- Tropical variations in longwave clear-sky feedback (e.g., “radiator fins”) are a consequence of this relative humidity dependence
- Cloud radiative effects estimated from a simple model do not qualitatively change this picture

Supporting Information:

Supporting Information may be found in the online version of this article.

Correspondence to:

B. A. McKim,
bam218@exeter.ac.uk

Citation:

McKim, B. A., Jeevanjee, N., & Vallis, G. K. (2021). Joint dependence of longwave feedback on surface temperature and relative humidity. *Geophysical Research Letters*, 48, e2021GL094074. <https://doi.org/10.1029/2021GL094074>

Received 26 APR 2021

Accepted 19 AUG 2021

Abstract Various studies have suggested that Earth’s clear-sky outgoing longwave radiation (OLR) varies linearly with surface temperature, with a longwave clear-sky feedback that is, independent of surface temperature and relative humidity. However, this uniformity conflicts with the notion that humidity controls tropical stability (e.g., the “furnace” and “radiator fins” of Pierrehumbert (1995, [https://doi.org/10.1175/1520-0469\(1995\)052%3C1784:TRFATL%3E2.0.CO;2](https://doi.org/10.1175/1520-0469(1995)052%3C1784:TRFATL%3E2.0.CO;2))). Here, we use a column model to explore the dependence of longwave clear-sky feedback on both surface temperature and relative humidity. We find that a strong humidity dependence in the feedback emerges above 275 K, which stems from the closing of the H₂O window, and that the furnace and radiator fins are consequences of this dependence. We then clarify that radiator fins are better characterized by tropical variations in clear-sky feedback than OLR. Finally, we construct a simple model for estimating the all-sky feedback and find that although clouds lower the magnitude of longwave feedback, the humidity-dependence persists.

Plain Language Summary The dependence of outgoing longwave radiation radiation on surface temperature (i.e., the feedback) is a major determinant of the climate’s stability. Various studies have suggested that the feedback is largely independent of both surface temperature and relative humidity, which implies that the climate stability is also independent of surface temperature and relative humidity. However, this uniformity seems to contradict other work which shows that the subtropics are relatively stable and the deep tropics are relatively unstable, implying the feedback must vary between the two regions. We resolve this apparent contradiction by systematically computing the feedback as a function of both surface temperature and relative humidity. Above 275 K, the feedback depends significantly on relative humidity. We then show the feedback does indeed vary in the tropics and that this difference arises from regional differences in relative humidity. Finally, we estimate the effects of clouds on the feedback with a simple model and find that although clouds have a destabilizing influence, the significant dependence on relative humidity persists. Our work gives a renewed appreciation for how the feedback can vary significantly with both surface temperature and relative humidity.

1. Introduction

The longwave clear-sky feedback parameter λ_{cs} relates a change in clear-sky outgoing longwave radiation OLR_{cs} to a change in surface temperature T_s ,

$$\lambda_{cs} \equiv \frac{dOLR_{cs}}{dT_s} \quad (\text{Wm}^{-2}\text{K}^{-1}). \quad (1)$$

It is a measure of the stability of the climate and thus is a well studied quantity, with a canonical value for its global mean of about $2.2 \pm 10\% \text{ Wm}^{-2}\text{K}^{-1}$ (Allan et al., 1999; Bony et al., 1995; Budyko, 1969; Cess et al., 1989, 1990; Chung et al., 2010; Dessler et al., 2008; Jeevanjee, 2018; Koll & Cronin, 2018; Raval et al., 1994; Zhang et al., 2020).

The convergence of the global mean value of λ_{cs} across both observations and the model hierarchy suggests robust physics that is, insensitive to the idiosyncrasies of the individual studies. Recently, Koll and Cronin (2018) gave an explanation of this physics as a balance between increasing surface Planck feedback and decreasing surface transmissivity. They verified that $\lambda_{cs} \approx 2.2 \text{ Wm}^{-2}\text{K}^{-1}$ for a wide range of T_s in a column model. Zhang et al. (2020) then extended this analysis to GCMs and similarly found λ_{cs} to be independent of both T_s and free-tropospheric relative humidity (RH).

© 2021. The Authors.

This is an open access article under the terms of the [Creative Commons Attribution License](https://creativecommons.org/licenses/by/4.0/), which permits use, distribution and reproduction in any medium, provided the original work is properly cited.

This work on the uniformity of feedback lies in tension with the notion that meridional variations in clear-sky relative humidity are important in controlling tropical stability. In particular, Pierrehumbert (1995) argued that the warm and moist deep tropics, with active deep convection (furnace) are close to a local runaway greenhouse, but are radiatively stabilized by the warm, yet dryer, and more quiescent subtropics (radiator fins). However, Pierrehumbert (1995) was equivocal on whether the furnace and radiator fins manifest as tropical variations in OLR_{cs} , or rather in λ_{cs} , which is the more relevant parameter for stability. Indeed, as we shall show later, the latitudinal variations in OLR_{cs} within the tropics are quite muted compared to OLR_{cs} variations over the globe. Here, then, we will pursue the idea that radiator fins manifest instead as tropical variations in λ_{cs} .

Clouds are another process that may play a role in controlling the structure of zonal-mean feedback. Pierrehumbert (1995) argued for the presence of tropical furnaces and radiator fins using only clear-sky physics. However, humid regions and cloudy regions often go hand-in-hand, and high clouds are known to have a robust influence on the longwave feedback (Zelinka & Hartmann, 2010), so we might expect the longwave all-sky feedback parameter λ_{as} to look different from λ_{cs} in the zonal mean.

We lack clarity on whether the taxonomy of the furnace and radiator fins are better described by OLR_{cs} or by λ_{cs} . There is also a tension between the constancy of λ_{cs} observed across studies and the notion that humidity variations control tropical stability, and it is unclear how clouds might modulate this relationship. This state of affairs motivates us to ask the following questions:

1. Do furnaces and radiator fins indeed manifest as a contrast in the zonal-mean λ_{cs} as opposed to the zonal-mean OLR_{cs} ?
2. How do we reconcile variations in λ_{cs} implied by furnaces and radiator fins when other studies suggest λ_{cs} is approximately constant?
3. How do clouds modify the meridional structure of longwave feedback?

To this end we first construct a “phase space,” in which λ_{cs} is computed as a joint function of T_s and column RH. Below 275 K, we find that λ_{cs} stays within 10% of $2.2 \text{ Wm}^{-2}\text{K}^{-1}$, even as RH varies. Above 275 K, however, a significant RH-dependence emerges, leading to much greater variations in λ_{cs} . We show that this RH-dependence stems from the closing of the H_2O window. The tropical contrast in zonal-mean λ_{cs} is, then, a consequence of this RH-dependence at high temperatures. Finally, we construct a simple model for evaluating the all-sky feedback and find that although clouds decrease the zonal-mean feedback, the RH-dependence remains significant.

2. Results

2.1. Exploring the State Dependence of λ_{cs}

We first address Question 2 by exploring the state dependence of λ_{cs} as a function of both T_s and RH. We use RH as a state variable because RH-based feedbacks have certain advantages over specific humidity (q_v) based feedbacks both from a thermodynamic point of view (Held & Shell, 2012) and from a radiative point of view (Jeevanjee et al., 2021), as specific humidity already has a de facto strong temperature dependence through the Clausius-Clapeyron relation. To compute radiative transfer we use PyRADS, a validated line-by-line column model (Koll & Cronin, 2019). We used the model in 1-D radiative-convective equilibrium, following Koll and Cronin (2018), in which a moist adiabat profile is assumed. We set the CO_2 concentration to 340 ppmv, the number of pressure levels to 30 (from 0.1 to 1,000 hPa), and consider a spectral range between 0.1 and $3,500 \text{ cm}^{-1}$ at 0.01 cm^{-1} resolution. We only then need to specify the surface temperature and a vertically uniform relative humidity to compute OLR_{cs} for the column. For more details of atmospheric structure and spectral databases, see “Materials and Methods” in Koll and Cronin (2018).

We calculate λ_{cs} in the following way. We first compute OLR_{cs} for some T_s and RH; we then perturb the surface temperature by an amount ΔT , and allow the moist-adiabatic atmosphere to respond while holding RH fixed; finally we calculate the perturbed OLR and take the finite difference between the two states. In summary:

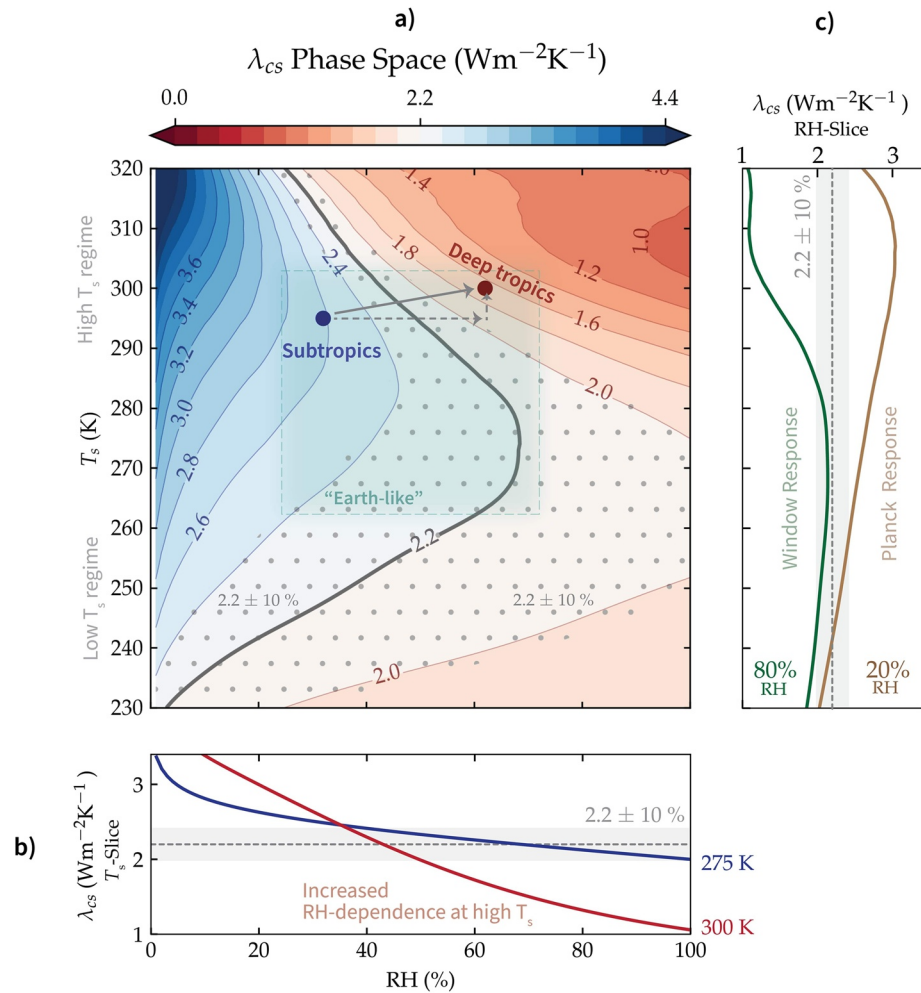


Figure 1. Exploration of state dependence of longwave clear-sky feedback λ_{cs} in a column model. (a) λ_{cs} phase space as a function of surface temperature T_s and column relative humidity RH, with contours indicating values of λ_{cs} and stipples indicating values between $2.2 \pm 10\% \text{ Wm}^{-2}\text{K}^{-1}$. See Equation 2 for details of the calculation. Typical temperatures and humidity ranges spanned by the Earth are shaded in green. The subtropics and deep tropics are noted as $\sim 295 \text{ K}/30\%$, and $\sim 300 \text{ K}/60\%$, respectively. The gray arrows indicate different pathways to move from the subtropics to the deep tropics. (b) Cross section of λ_{cs} phase space at 275 and 300 K (c) Cross section of λ_{cs} phase space at 20% and 80% relative humidity.

$$\lambda_{cs}(T_s, \text{RH}) \approx \frac{\text{OLR}_{cs}(T_s + \Delta T, \text{RH}) - \text{OLR}_{cs}(T_s, \text{RH})}{\Delta T}, \quad (2)$$

where $\Delta T = 1 \text{ K}$ in our calculations. Note that the Planck, lapse rate, and water vapor feedbacks are included in λ_{cs} . The moist adiabat is not satisfied in the mid-latitudes, but we note that the lapse rate feedback is small when RH is fixed (Cess, 1975; Held & Shell, 2012; Jeevanjee et al., 2021; Zelinka et al., 2020). We exclude the RH-feedback associated with a change in RH with surface warming for simplicity and because its value in the global mean is $< 0.1 \text{ Wm}^{-2}\text{K}^{-1}$ (Held & Shell, 2012; Zelinka et al., 2020). We also assume the atmosphere responds like a moist adiabat for simplicity, although in reality the atmospheric temperature change is not always due to a local T_s change (Mauritsen, 2016). We give some perspective on our feedback analysis in Section 3.1.

Our results are summarized in Figure 1a for surface temperatures between 230 and 320 K and relative humidities between 0% and 100%. We identify 275 K as the de facto boundary between a low temperature regime and a high temperature regime because each region exhibits distinct behaviors for λ_{cs} . Below 275 K, there is a very small RH-dependence — for values of RH between 20% and 80%, λ_{cs} remains within 10% of

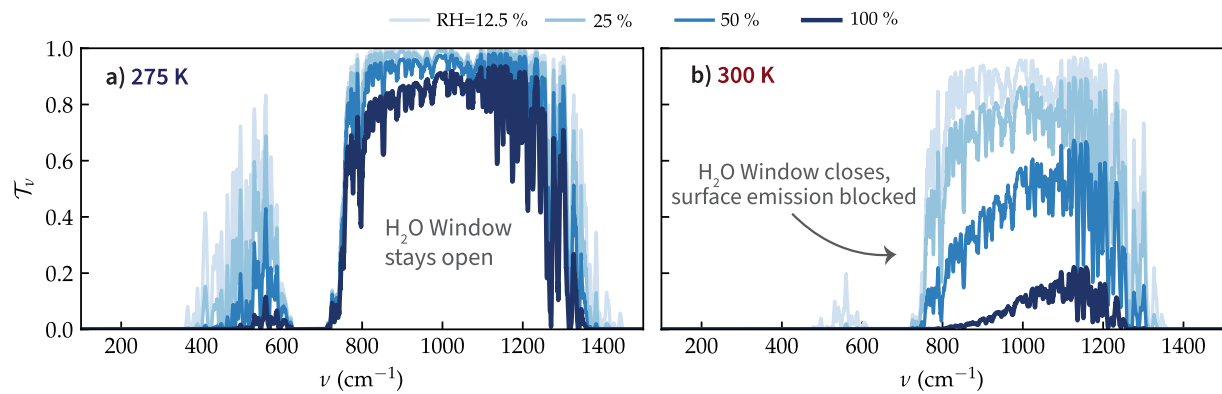


Figure 2. The closing of the H₂O window is sensitive to relative humidity at high surface temperatures. The surface-to-space transmission T_v is plotted as a function of wavenumber ν for a surface temperature of 275 K (a) and 300 K (b), and a relative humidity of 12.5%, 25%, 50%, and 100%. The H₂O window is where $T_v \approx 1$ and surface emission escapes directly to space. We use a Savitzky–Golay filter with a 5 cm^{-1} width to smooth these plots.

$2.2 \text{ Wm}^{-2}\text{K}^{-1}$. Above 275 K, however, a significant RH-dependence emerges: the value of λ_{cs} differs from $2.2 \text{ Wm}^{-2}\text{K}^{-1}$ by much more than 10% over the same range of humidity. We explicitly plot the RH-dependence of λ_{cs} at 275 and 300K (Figure 1b) to highlight this difference in behavior. The majority of “Earth-like” values of (T_s, RH) pairs fall within 10% of $2.2 \text{ Wm}^{-2}\text{K}^{-1}$ (indicated by the overlap between the boxed and stippled areas in Figure 1a). Thus, in response to Question 2, a λ_{cs} value of $2.2 \text{ Wm}^{-2}\text{K}^{-1}$ will occur over much of the globe, and in particular will manifest as the constant slope of an OLR_{cs} versus T_s regression, as in Figure 1 of Koll and Cronin (2018). Nonetheless, Figure 1 shows that λ_{cs} can still vary considerably at the higher temperatures of Earth’s tropics.

2.2. Importance of the H₂O Window

This section provides additional context about λ_{cs} by focusing on the underlying radiation physics that controls the climate response.

Since λ_{cs} is dominated by surface emission through the H₂O window (Koll & Cronin, 2018), the wavenumbers at which H₂O absorption is negligible for surface emission, we expect the window to play an important role in the RH-dependence of λ_{cs} at high temperatures. To display the H₂O window, we plot the surface-to-space transmission T_v , which measures the portion of surface emission at wavenumber ν that escapes to space. At a surface temperature of 275 K (Figure 2a), the H₂O window remains open as the relative humidity is increased from 12.5% to 100%. At a surface temperature of 300 K (Figure 2b), however, the H₂O window closes rapidly as the relative humidity is increased from 12.5% to 100%. This is due to activation of H₂O continuum absorption (Koll & Cronin, 2018). Thus relative humidity variations are sufficient to close the H₂O window, but only at high temperatures.

Koll and Cronin (2018) emphasized the robustness of $\lambda_{cs} \approx 2.2 \text{ Wm}^{-2}\text{K}^{-1}$ as arising from a balance between the closing of the H₂O window and the nonlinear $4\sigma T_s^3$ surface Planck feedback. However, at high temperatures this balance is not as robust, as evidenced by the decreasing width of the stippled area of the λ_{cs} phase space, which denotes $\lambda_{cs} = 2.2 \pm 10\% \text{ Wm}^{-2}\text{K}^{-1}$, with increasing temperature (Figure 1a). The balance is not as robust because the H₂O window closes much faster with temperature at 100% RH than at 20% RH (Figure 2b), leading to a “Planck-dominated” response at low RH, and a “window-dominated” response at high RH (Figure 1c).

2.3. Tropical Variations in λ_{cs}

In Question 1 we asked whether the furnaces and radiator fins described in Pierrehumbert (1995) manifest as a contrast in the zonal-mean λ_{cs} as opposed to the zonal-mean OLR_{cs} . To answer this question we will first compute time- and zonal-mean T_s and RH from ERA5 reanalysis (Hersbach et al., 2020) and use these values to read off zonal-mean λ_{cs} from the phase space of Figure 1. We take hourly data sub-sampled every 6 h from January 1 to December 31, 1981 and compute annual averages. Following Zhang et al. (2020),

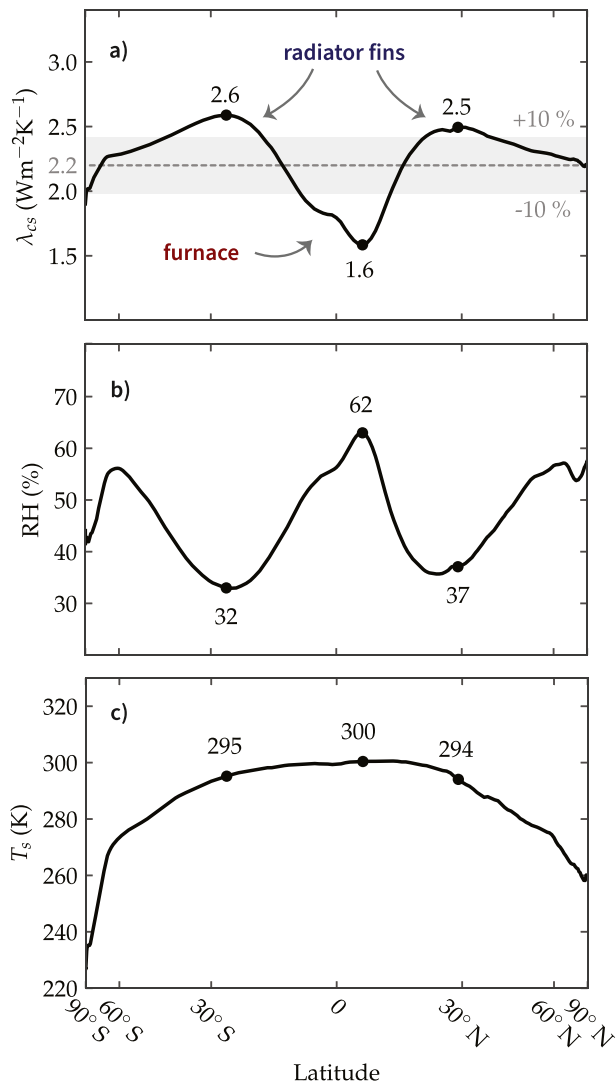


Figure 3. Furnaces and radiator fins manifest as meridional variations in longwave clear-sky feedback λ_{cs} . (a) Zonal-mean λ_{cs} is diagnosed from Figure 1, using the reanalysis zonal-mean relative humidity (RH) (b) and the reanalysis zonal-mean T_s (c) as inputs (see text for details). The shaded region in (a) represents the global mean value of $2.2 \pm 10\% \text{ Wm}^{-2}\text{K}^{-1}$ reported in other studies. We posit that the local maxima and minimum of λ_{cs} that lie outside this range should be considered the “radiator fins” and “furnace,” respectively, of the tropics. Note the equal-area scaling of the x-axis.

we calculate a free-tropospheric column RH as the water vapor mass between 850 and 300 hPa, divided by the saturated water vapor mass within the column. We exclude the boundary layer RH and stratospheric water vapor because of their limited impact on the OLR (Zhang et al., 2020).

We might expect a significant drop in λ_{cs} from the subtropics to the deep tropics by looking at representative values of T_s and RH in the λ_{cs} -phase space (Figure 1). Indeed, the meridional structure of zonal-mean λ_{cs} calculated as described above, shows that λ_{cs} varies from 2.6 to 1.6 $\text{Wm}^{-2}\text{K}^{-1}$ in the tropics, a 38% drop (Figure 3a). Both the subtropical maxima and deep tropical minimum lie outside the $2.2 \pm 10\% \text{ Wm}^{-2}\text{K}^{-1}$ range. We posit that these extrema of λ_{cs} should be considered the true “radiator fins” and “furnace,” respectively, of the tropics.

We can test whether the significant drop in λ_{cs} between the radiator fins and the furnace is due to the difference in humidity, as emphasized by Pierrehumbert (1995), or if the drop is due to the difference in temperature. If we look again at the phase space in Figure 1, we can take a path that goes from the subtropics to the deep tropics in two parts (the order does not matter): a first part with constant surface temperature, and a second part with constant relative humidity (see the dashed gray arrows). In this region of phase space, the doubling of relative humidity from 30% to 60% causes a much larger change in λ_{cs} than the increase in surface temperature from 295 to 300 K does.

Our answer to the first part of Question 1 is then: zonal-mean λ_{cs} exhibits local extrema, which may be usefully viewed as the “furnace” and “radiator fins” of the tropics. Furthermore, these extrema are indeed due to RH variations, consistent with Pierrehumbert (1995). λ_{cs} exhibits a local maxima in the subtropics because they are hot and dry enough for the feedback to exhibit a Planck-dominated response, and λ_{cs} exhibits a local minimum in the deep tropics because they are hot and moist enough for the feedback to exhibit a window-dominated response (Figure 1c).

To answer the second part of Question 1, that is, why radiator fins should not be regarded as a contrast in the zonal-mean OLR_{cs} , we plot the annual- and zonal-mean OLR_{cs} and OLR_{as} from ERA5 reanalysis in gray in Figures 4c and 4d. Note the muted latitudinal variations of OLR_{cs} within the tropics ($\sim 10 \text{ Wm}^{-2}$) compared to variations in OLR_{cs} throughout the rest of the globe ($\sim 100 \text{ Wm}^{-2}$). This muted latitudinal dependence within the tropics is inconsistent with the notion of radiator fins as significant subtropical maxima in OLR_{cs} , which is why we focus on λ_{cs} instead. OLR_{as} does have more significant subtropical extrema, but these should not be interpreted as a furnace and radiator fins because the longwave warming effect of deep tropical clouds is balanced by their shortwave cooling effect (Hartmann & Berry, 2017; Pierrehumbert, 1995).

2.4. Incorporating the Effects of Cloudiness

In Question 3, we asked whether clouds affect the meridional structure in zonal-mean longwave feedback in the tropics. Rather than explicitly compute cloud feedbacks, which is beyond the scope of this study, we try to estimate them by constructing a simple model for how clouds modify longwave emission. To validate the approach, we first estimate the all-sky OLR, OLR_{as} , from a few inputs: OLR_{cs} , the cloud top fraction f , and the cloud top temperature T_{ct} . OLR_{cs} is taken directly from ERA5 reanalysis. f is diagnosed from ERA5 reanalysis as the local max of the zonal-mean cloud fraction profile above a 550 hPa threshold, which is used to avoid misidentifying cloud tops with boundary layer cloudiness. T_{ct} is the atmospheric temperature

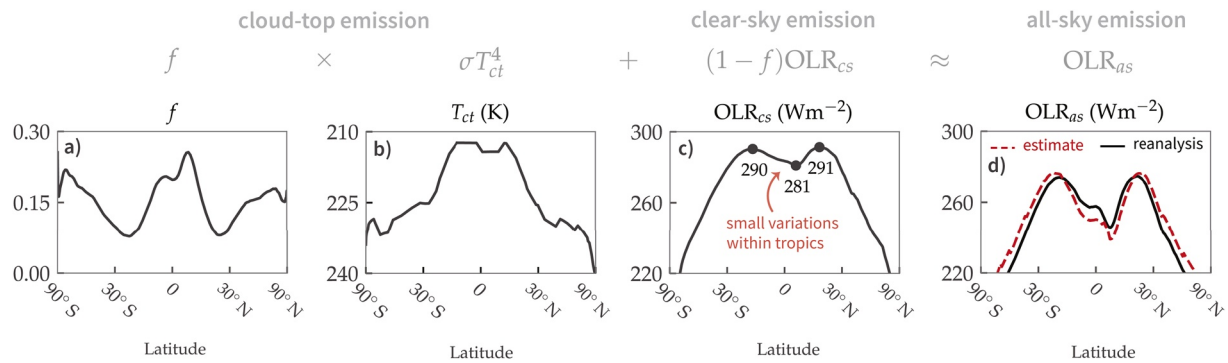


Figure 4. A simple model for zonal-mean all-sky emission. (a) cloud top fraction f , (b) cloud top temperature T_{ct} , (c) clear-sky emission OLR_{cs} , and (d) all-sky emission OLR_{as} . The black curves are from ERA5 reanalysis. The dashed-red curve in (d) is our simple estimate produced by the equation above the panels (see Equation 3). Note the equal-area scaling of the x-axis.

at which cloud fraction profile peaks. We smooth T_{ct} with a Savitzky-Golay filter with a 10° latitude width to account for sharp jumps in T_{ct} arising from the limited vertical resolution. This method of identifying cloud tops is similar to Thompson et al. (2017). We show our methodology in the Supporting Information S1.

To estimate OLR_{as} , we first consider the effect of high clouds, which block longwave emission from lower levels and replace it with their own longwave emission from cloud tops. We assume high cloud emission acts like a black body and occurs high enough in the atmosphere that emission travels directly to space (Siebesma et al., 2020). As for low clouds, we grossly assume the low clouds emit at a temperature close enough to T_s that they only negligibly alter the outgoing radiation (Hartmann, 2015). Given these assumptions, we can now write down a simple expression for OLR_{as} :

$$OLR_{as} \approx \sigma T_{ct}^4 f + OLR_{cs}(1 - f). \quad (3)$$

This model is similar in some ways to the conceptual model created in Soden et al. (2008) to examine cross-field correlations between clear-sky and cloud feedbacks.

To get a sense of what the inputs to Equation 3 look like, we plot annual- and zonal-mean f , T_{ct} , OLR_{cs} , and OLR_{as} from ERA5 reanalysis in gray in Figure 4. We test the approximate all-sky radiation from Equation 3 against OLR_{as} directly output from ERA5 analysis, which includes cloud opacities and comprehensive radiative transfer in its calculation. We find that our model does an acceptable job in replicating the reanalysis (Figure 4d), although there is a slight underestimate within the tropics and a slight overestimate outside the tropics. Overall, the relative accuracy and physical transparency of our estimate gives us enough confidence in this model to proceed.

We now use Equation 3 to compute the longwave all-sky feedback, λ_{as} . We aim to assess the order of magnitude impact of clouds on our findings, so we first assume high cloud temperatures do not change appreciably with warming, consistent with the fixed anvil temperature (FAT) hypothesis (Hartmann & Larson, 2002; Zelinka & Hartmann, 2010). We assume a FAT as opposed to a proportionally higher anvil temperature (PHAT) to explore a well-defined limit of the high cloud altitude feedback. Although f can change with warming (Bony et al., 2016; Saint-Lu et al., 2020), the high cloud area feedback is quite uncertain (Sherwood et al., 2020; Wing et al., 2020), so for simplicity we assume f is constant with warming. Differentiating Equation 3 with respect to T_s yields:

$$\lambda_{as} = \lambda_{cs}(1 - f). \quad (4)$$

This equation makes it conceptually clear how clouds modify λ_{cs} : the longwave feedback over clouds is 0. Since f is positive definite (Figure 4), $\lambda_{as} \leq \lambda_{cs}$, which is well demonstrated in the in the zonal mean in Figure 5a. The all-sky feedback looks like a simple translation downward of the clear-sky feedback, and there is still a significant (~50%) variation in λ_{as} from the subtropics to the deep tropics. Our answer to Question 3 is then: Clouds have a destabilizing influence on the longwave feedback. However, the structure of all-sky feedback looks similar to clear-sky feedback, implying that the RH-dependence from clear-sky effects still dominates the meridional structure.

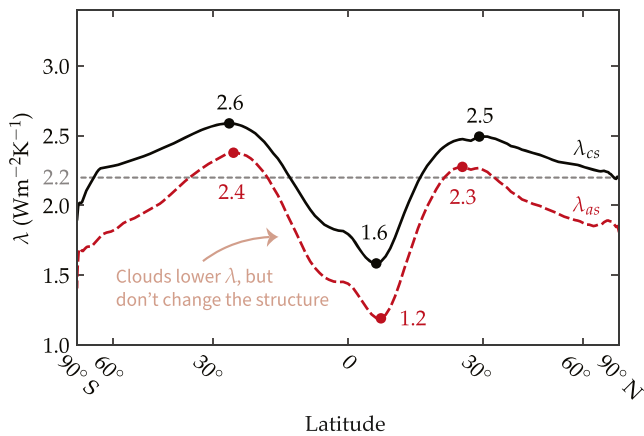


Figure 5. Incorporating clouds into the longwave feedback. Zonal-mean all-sky feedback (λ_{as} , dashed-red) is diagnosed from zonal-mean clear-sky feedback (λ_{cs} , solid-black) and zonal-mean cloud top fraction f . See Equation 4 for details. Note the equal-area scaling of the x-axis.

3. Discussion

Our work can be summarized as follows:

1. At high temperatures, variations in RH are sufficient to close the H₂O window, driving deviations in λ_{cs} from the typical value of 2.2 Wm⁻²K⁻¹ (Figure 1).
2. Furnaces and radiator fins can be interpreted as tropical extrema in zonal-mean λ_{cs} as a consequence of the RH-dependence (Figure 3). They should not be interpreted as significant tropical extrema in zonal-mean OLR_{cs} because tropical variations in OLR_{cs} are small compared to global variations in OLR_{cs} (Figure 4c).
3. Cloud radiative effects can be estimated with a simple equation to reconstruct the all-sky OLR (Figure 4), which we then use to estimate the all-sky feedback. Clouds lower the feedback relative to clear skies, but the RH-dependence of the feedback remains significant (Figure 5).

3.1. Comparison to Other Work

We have demonstrated a reason for why a large contrast in λ_{cs} emerges in the tropics, but our results for the zonal-mean feedback cannot be directly compared to most other studies of regional feedback (e.g., Armour et al., 2013 and Feldl & Roe, 2013a, 2013b). Our clear-sky feedback λ_{cs} is not equal to the sum of the Planck, lapse rate, and water vapor feedbacks, because these feedbacks include “cloud climatological effects” (Yoshimori et al., 2020), that is, these feedbacks are calculated in the presence of clouds from the control simulation. Furthermore, our all-sky feedback λ_{as} is also not equal to this sum of conventional feedbacks, because those feedbacks fix the cloud pressure, whereas we fix the cloud temperature. These issues were discussed in detail by Yoshimori et al. (2020), and our λ_{as} should be comparable to their T-FRAT feedback in which the RH and cloud temperatures are fixed. Further work could explicitly explore such comparisons.

Our results can still be fruitfully compared to Zhang et al. (2020), who also analyzed the zonal-mean λ_{cs} in GCMs, but without the assumptions that column RH is fixed with warming and that the atmosphere follows a moist adiabat. We both find a drop in λ_{cs} of ~ 1 Wm⁻²K⁻¹ from the subtropics to the deep tropics. However, Zhang et al. (2020) suggested that the drop in zonal mean λ_{cs} results from the RH-feedback due to local column RH increases with surface warming. Column RH is fixed in our study and yet we still get a significant tropical dip, although our λ_{cs} is offset by a constant ~ 0.5 Wm⁻²K⁻¹ from their results. This comparison suggests that climatological RH causes the tropical variations in λ_{cs} , whereas the RH-feedback and deviations from a moist adiabat uniformly lowers λ_{cs} . The importance of climatological RH is further supported by Bourdin et al. (2021), who also finds that climatological RH influences climate sensitivity, even if the vertical distribution of RH remains unchanged with warming.

Analyzing feedbacks locally or globally can give opposing impressions to the radiative response to warming. Local surface warming in the deep tropics yields a small, local OLR increase (as measured by λ_{cs} and λ_{as}) but a large, global OLR increase (Dong et al., 2019). The discrepancy between the weak, local and the strong, global radiative response from warming the deep tropics arises from atmospheric temperature changes not associated with a local T_s change, that is, the remote warming of the free troposphere (Ceppi et al., 2017; Mauritsen, 2016). A local feedback analysis, by construction, cannot capture the effects of remote warming, which should be noted when comparing results across studies. The relative contributions of local surface warming versus non-local free-tropospheric warming to OLR change is relatively unexplored, so further study might alter our characterization of the tropical radiative response if one contribution can be shown to dominate over the other.

Our new understanding of the state dependence of λ_{cs} gives context to previous results. For example, Bloch-Johnson et al. (2021) and Meraner et al. (2013) attributed an increase in equilibrium climate sensitivity to the decrease in λ_{cs} with warming. We expect these variations in λ_{cs} to be enhanced in climates

hotter than present-day Earth and conversely to be suppressed in climates cooler than present-day Earth. Our particular calculation of the λ_{cs} phase space assumed that the CO₂ concentration is fixed at 340 ppmv, which neglects the increasingly important role of CO₂ in stabilizing the climate at high CO₂ concentrations (Seeley & Jeevanjee, 2020). However, the strength in our approach of studying the joint dependence of λ_{cs} on T_s and RH is its generality, for our approach cannot only be applied to our present-day climate, but to past climates like the Eocene, Pliocene, and Last Glacial Maximum, and to future climates predicted from different RCP scenarios.

Data Availability Statement

ERA5 data are available from <https://doi.org/10.24381/cds.bd0915c6>. Data from the PyRADS calculations are available from <https://zenodo.org/record/5164050#.YQwWf1NKhZ1>.

Acknowledgments

This work was funded by CEMPS at the University of Exeter. The authors thank two anonymous reviewers for their constructive comments, which have greatly improved the manuscript. The authors also thank Penelope Maher, Stephen Thomson, Hugo Lambert, and Mitchell Koerner for their helpful conversations on this project.

References

- Allan, R. P., Shine, K. P., Slingo, A., & Pammitt, J. A. (1999). The dependence of clear-sky outgoing long-wave radiation on surface temperature and relative humidity. *Quarterly Journal of the Royal Meteorological Society*, *125*(558), 2103–2126. <https://doi.org/10.1002/qj.49712555809>
- Armour, K. C., Bitz, C. M., & Roe, G. H. (2013). Time-varying climate sensitivity from regional feedbacks. *Journal of Climate*, *26*(13), 4518–4534. <https://doi.org/10.1175/JCLI-D-12-00544.1>
- Bloch-Johnson, J., Rugenstein, M., Stolpe, M. B., Rohrschneider, T., Zheng, Y., & Gregory, J. M. (2021). Climate sensitivity increases under higher CO₂ levels due to feedback temperature dependence. *Geophysical Research Letters*, *48*(4), e2020GL089074. <https://doi.org/10.1029/2020GL089074>
- Bony, S., Duvel, J., & Le Trent, H. (1995). Observed dependence of the water vapor and clear-sky greenhouse effect on sea surface temperature: Comparison with climate warming experiments. *Climate Dynamics*, *11*, 307–320. <https://doi.org/10.1007/BF00211682>
- Bony, S., Stevens, B., Coppin, D., Becker, T., Reed, K. A., Voigt, A., & Medeiros, B. (2016). Thermodynamic control of anvil cloud amount. *Proceedings of the National Academy of Sciences*, *113*(32), 8927–8932. <https://doi.org/10.1073/pnas.1601472113>
- Bourdin, S., Kluff, L., & Stevens, B. (2021). Dependence of climate sensitivity on the given distribution of relative humidity. *Geophysical Research Letters*, *48*(8), e2021GL092462. <https://doi.org/10.1029/2021GL092462>
- Budyko, M. I. (1969). The effect of solar radiation variations on the climate of the Earth. *Tellus*, *21*(5), 611–619. <https://doi.org/10.1111/j.2153-3490.1969.tb00466.x>
- Ceppi, P., Briant, F., Zelinka, M. D., & Hartmann, D. L. (2017). Cloud feedback mechanisms and their representation in global climate models. *WIREs Climate Change*, *8*(4), e465. <https://doi.org/10.1002/wcc.465>
- Cess, R. (1975). Global climate change: An investigation of atmospheric feedback mechanisms. *Tellus*, *27*(3), 193–198. <https://doi.org/10.1111/j.2153-3490.1975.tb01672.x>
- Cess, R. D., Potter, G. L., Blanchet, J. P., Boer, G. J., Del Genio, A. D., Déqué, M., & Zhang, M.-H. (1990). Intercomparison and interpretation of climate feedback processes in 19 atmospheric general circulation models. *Journal of Geophysical Research*, *95*(D10), 16601–16615. <https://doi.org/10.1029/JD095iD10p16601>
- Cess, R. D., Potter, G. L., Blanchet, J. P., Boer, G. J., Ghan, S. J., Kiehl, J. T., & Yagai, I. (1989). Interpretation of cloud-climate feedback as produced by 14 atmospheric general circulation models. *Science*, *245*(4917), 513–516. <https://doi.org/10.1126/science.245.4917.513>
- Chung, E.-S., Yeomans, D., & Soden, B. J. (2010). An assessment of climate feedback processes using satellite observations of clear-sky olr. *Geophysical Research Letters*, *37*(2), L02702. <https://doi.org/10.1029/2009GL041889>
- Dessler, A. E., Yang, P., Lee, J., Solbrig, J., Zhang, Z., & Minschwaner, K. (2008). An analysis of the dependence of clear-sky top-of-atmosphere outgoing longwave radiation on atmospheric temperature and water vapor. *Journal of Geophysical Research*, *113*(D17), D17102. <https://doi.org/10.1029/2008JD010137>
- Dong, Y., Proistosescu, C., Armour, K. C., & Battisti, D. S. (2019). Attributing Historical and future evolution of radiative feedbacks to regional warming patterns using a Green's function approach: The preeminence of the Western Pacific. *Journal of Climate*, *32*, 5471–5491. <https://doi.org/10.1175/JCLI-D-18-0843.1>
- Feldl, N., & Roe, G. H. (2013a). Four perspectives on climate feedbacks. *Geophysical Research Letters*, *40*(15), 4007–4011. <https://doi.org/10.1002/grl.50711>
- Feldl, N., & Roe, G. H. (2013b). The nonlinear and nonlocal nature of climate feedbacks. *Journal of Climate*, *26*(21), 8289–8304. <https://doi.org/10.1175/JCLI-D-12-00631.1>
- Hartmann, D. (2015). *Global physical climatology*. Elsevier Science. Retrieved from <https://books.google.co.uk/books?id=RsScBAAQBAJ>
- Hartmann, D. L., & Berry, S. E. (2017). The balanced radiative effect of tropical anvil clouds. *Journal of Geophysical Research: Atmospheres*, *122*(9), 5003–5020. <https://doi.org/10.1002/2017JD026460>
- Hartmann, D. L., & Larson, K. (2002). An important constraint on tropical cloud - Climate feedback. *Geophysical Research Letters*, *29*(20), 12-1–12-4. <https://doi.org/10.1029/2002GL015835>
- Held, I. M., & Shell, K. M. (2012). Using relative humidity as a state variable in climate feedback analysis. *Journal of Climate*, *25*(8), 2578–2582. <https://doi.org/10.1175/JCLI-D-11-00721.1>
- Hersbach, H., Bell, B., Berrisford, P., Hirahara, S., Horányi, A., Muñoz-Sabater, J., & Thépaut, J.-N. (2020). The ERA5 global reanalysis. *Quarterly Journal of the Royal Meteorological Society*, *146*(730), 1999–2049. <https://doi.org/10.1002/qj.3803>
- Jeevanjee, N. (2018). *The physics of climate change: Simple models in climate science*. Retrieved from <http://arxiv.org/abs/1802.02695>
- Jeevanjee, N., Koll, D. D. B., & Lutsko, N. (2021). “simpson's law” and the spectral cancellation of climate feedbacks. *Geophysical Research Letters*, *48*(14), e2021GL093699. <https://doi.org/10.1029/2021GL093699>
- Koll, D. D. B., & Cronin, T. W. (2018). Earth's outgoing longwave radiation linear due to H₂O greenhouse effect. *Proceedings of the National Academy of Sciences*, *115*(41), 10293–10298. <https://doi.org/10.1073/pnas.1809868115>
- Koll, D. D. B., & Cronin, T. W. (2019). *PyRADS: Python RADIation model for planetary atmosphereS*.

- Mauritsen, T. (2016). Clouds cooled the Earth. *Nature Geoscience*, 9(12), 865–867. <https://doi.org/10.1038/ngeo2838>
- Meraner, K., Mauritsen, T., & Voigt, A. (2013). Robust increase in equilibrium climate sensitivity under global warming. *Geophysical Research Letters*, 40(22), 5944–5948. <https://doi.org/10.1002/2013GL058118>
- Pierrehumbert, R. T. (1995). Thermostats, radiator fins, and the local runaway greenhouse. *Journal of Atmospheric Sciences*, 52(10), 1784–1806. [https://doi.org/10.1175/1520-0469\(1995\)052<1784:TRFATL>2.0.CO;2](https://doi.org/10.1175/1520-0469(1995)052<1784:TRFATL>2.0.CO;2)
- Raval, A., Oort, A. H., & Ramaswamy, V. (1994). Observed dependence of outgoing longwave radiation on sea surface temperature and moisture. *Journal of Climate*, 7(5), 807–821. [https://doi.org/10.1175/1520-0442\(1994\)007<0807:ODOOLR>2.0.CO;2](https://doi.org/10.1175/1520-0442(1994)007<0807:ODOOLR>2.0.CO;2)
- Saint-Lu, M., Bony, S., & Dufresne, J.-L. (2020). Observational evidence for a stability iris effect in the tropics. *Geophysical Research Letters*, 47(14), e2020GL089059. <https://doi.org/10.1029/2020GL089059>
- Seeley, J. T., & Jeevanjee, N. (2020). H₂O windows and CO₂ radiator fins: A clear-sky explanation for the peak in equilibrium climate sensitivity. *Geophysical Research Letters*, 48(4), e2020GL089609. <https://doi.org/10.1029/2020GL089609>
- Sherwood, S. C., Webb, M. J., Annan, J. D., Armour, K. C., Forster, P. M., Hargreaves, J. C., & Zelinka, M. D. (2020). An assessment of earth's climate sensitivity using multiple lines of evidence. *Reviews of Geophysics*, 58(4), e2019RG000678. <https://doi.org/10.1029/2019RG000678>
- Siebesma, A., Bony, S., Jakob, C., & Stevens, B. (2020). *Clouds and climate: Climate science's greatest challenge*. Cambridge University Press. Retrieved from <https://books.google.co.uk/books?id=rvXvDwAAQBAJ>
- Soden, B. J., Held, I. M., Colman, R., Shell, K. M., Kiehl, J. T., & Shields, C. A. (2008). Quantifying climate feedbacks using radiative kernels. *Journal of Climate*, 21(14), 3504–3520. <https://doi.org/10.1175/2007JCLI2110.1>
- Thompson, D. W. J., Bony, S., & Li, Y. (2017). Thermodynamic constraint on the depth of the global tropospheric circulation. *Proceedings of the National Academy of Sciences*, 114(31), 8181–8186. <https://doi.org/10.1073/pnas.1620493114>
- Wing, A. A., Stauffer, C. L., Becker, T., Reed, K. A., Ahn, M.-S., Arnold, N. P., & Zhao, M. (2020). Clouds and convective self-aggregation in a multimodel ensemble of radiative-convective equilibrium simulations. *Journal of Advances in Modeling Earth Systems*, 12(9), e2020MS002138. <https://doi.org/10.1029/2020MS002138>
- Yoshimori, M., Lambert, F. H., Webb, M. J., & Andrews, T. (2020). Fixed anvil temperature feedback: Positive, zero, or negative? *Journal of Climate*, 33(7), 2719–2739. <https://doi.org/10.1175/JCLI-D-19-0108.1>
- Zelinka, M. D., & Hartmann, D. L. (2010). Why is longwave cloud feedback positive? *Journal of Geophysical Research*, 115(D16), D16117. <https://doi.org/10.1029/2010JD013817>
- Zelinka, M. D., Myers, T. A., McCoy, D. T., Po-Chedley, S., Caldwell, P. M., Ceppi, P., & Taylor, K. E. (2020). Causes of higher climate sensitivity in CMIP6 models. *Geophysical Research Letters*, 47(1), e2019GL085782. <https://doi.org/10.1029/2019GL085782>
- Zhang, Y., Jeevanjee, N., & Fueglistaler, S. (2020). Linearity of outgoing longwave radiation: From an atmospheric column to global climate models. *Geophysical Research Letters*, 47(17), e2020GL089235. <https://doi.org/10.1029/2020GL089235>